# Kinetic Mechanism of Glutaryl-CoA Dehydrogenase†

K. Sudhindra Rao,‡ Mark Albro,‡ Timothy M. Dwyer,|| and Frank E. Frerman*,‡,§

*Departments of Pediatrics and Pharmaceutical Sciences, University of Colorado at Denver and Health Sciences Center, 12800 East Nineteenth Avenue, P18-4404B, Mail Stop 8313, P.O. Box 6511, Aurora, Colorado 80045-0511, and Department of Chemistry, Towson University, Towson, Maryland 21252*

*Received May 5, 2006; Revised Manuscript Received October 5, 2006*

ABSTRACT: Glutaryl-CoA dehydrogenase (GCD) is a homotetrameric enzyme containing one noncovalently bound FAD per monomer that oxidatively decarboxylates glutaryl-CoA to crotonyl-CoA and $CO_2$. GCD belongs to the family of acyl-CoA dehydrogenases that are evolutionarily conserved in their sequence, structure, and function. However, there are differences in the kinetic mechanisms among the different acyl-CoA dehydrogenases. One of the unanswered aspects is that of the rate-determining step in the steady-state turnover of GCD. In the present investigation, the major rate-determining step is identified to be the release of crotonyl-CoA product because the chemical steps and reoxidation of reduced FAD are much faster than the turnover of the wild-type GCD. Other steps are only partially rate-determining. This conclusion is based on the transit times of the individual reactions occurring in the active site of GCD.

The oxidative decarboxylation of glutaryl-CoA catalyzed by the flavoprotein, glutaryl-CoA dehydrogenase (GCD),[1] is a common reaction in the mitochondrial oxidation of lysine, tryptophan, and hydroxylysine (*1*). The reductive half-reaction of the dehydrogenase flavin yields the enzyme-bound intermediate, glutaconyl-CoA, which is subsequently decarboxylated to yield crotonyl-CoA and $CO_2$ (*1*, *2*). Several aspects of the chemical mechanism of GCD have been addressed including (a) the identity of the catalytic base (*3*), (b) the function of Arg94 in catalysis (*4*), (c) the identification of glutaconyl-CoA as an enzyme-bound intermediate (*2*), (d) the crystal structure of GCD with and without bound ligand (*5*), and (e) participation of water in catalysis (*6*). These studies laid the foundation to explore the kinetic mechanism of GCD and identify the rate-determining step(s) in the turnover of the dehydrogenase.

Steady-state deuterium kinetic isotope effects and transient state kinetics of individual chemical steps are common approaches to identify the rate-determining step of an enzyme under steady-state conditions (*7*, *8*). In this communication, we have identified the rate-determining step in the overall reaction pathway of GCD. The elementary chemical steps catalyzed by wild-type GCD, in sequence, are (a) abstraction of the α-proton of the substrate by the catalytic base, Glu370, (b) hydride transfer from the *β*-carbon of the substrate to the N(5) of the FAD, (c) decarboxylation of the enzyme-bound intermediate, glutaconyl-CoA, by breakage of C*γ*−C*δ* bond, resulting in formation of a crotonyl-CoA dienolate anion and $CO_2$, and (d) protonation at C*γ* of the crotonyl-CoA dienolate intermediate, resulting in the product, crotonyl-CoA. FAD is the electron acceptor in the oxidation of the substrate. Reoxidation of the dehydrogenase flavin occurs in two $1e^-$ steps by an external electron acceptor to complete the catalytic cycle. The physical steps involved in the catalytic cycle are (a) binding of the substrate and (b) release of the products: crotonyl-CoA, $CO_2$, and a proton. A proton is formed when ferrocenium dye is used as an external electron acceptor. Scheme 1 shows the sequence of the chemical steps (*6*). These steps are essentially the same in the other members of acyl-CoA dehydrogenase family except for the decarboxylation of glutaconyl-CoA, the enzyme-bound product of glutaryl-CoA oxidation (*9*). Experiments were carried out with wild-type GCD to develop methods that may be used to investigate the role of active site residues in catalysis. The data indicate that the chemical steps and the two $1e^-$ transfer steps are faster than steady-state turnover catalyzed by wild-type GCD, suggesting that crotonyl-CoA release from the enzyme is the predominant rate-determining step. Similarly, in the decarboxylation reaction catalyzed by GCD, crotonyl-CoA release is the predominant rate-determining step. These conclusions are based on the determination of "net rate constants" in the forward direction and summing the transit times for all the steps (*10*).

## EXPERIMENTAL METHODS

*Enzymes and Reagents.* Acetyl-CoA, crotonyl-CoA, and glutaryl-CoA were purchased from Sigma. Ferrocenium hexafluorophosphate ($FcPF_6$), dimethyl 3-hydroxyglutarate, and glutaconic acid were purchased from Aldrich. Thiodiglycolic anhydride was purchased from Lancaster. 2,2,4,4-$d_4$-glutaric acid (99% D), 2,2,3,3,4,4-$d_6$-glutaric acid (99% D) were obtained from C/D/N Isotopes Inc., Canada. L-3-Hydroxybutyryl-CoA was synthesized from crotonyl-CoA using rat liver crotonase as described previously (*2*, *11*). Dimethyl 3-hydroxyglutarate was saponified with 2 equiv of sodium hydroxide by refluxing for 30 min to yield

† This work was supported by grants from the National Institutes of Health (NS39339) and from the Childrens' Hospital Research Foundation to F.E.F.

* Corresponding author. E-mail: Frank.Frerman@UCHSC.edu. Phone: 1-303-724-3809. Fax: 1-303-724-3838.

‡ Department of Pediatrics.

§ Department of Pharmaceutical Sciences.

|| Department of Chemistry.

[1] Abbreviations: GCD, glutaryl-CoA dehydrogenase; $FcPF_6$, ferrocenium hexafluorophosphate; QSAR, quantitative-structure activity relationships; HPLC, high-performance liquid chromatography; EDTA, ethylenediamine tetraacetic acid, $2Na^+$ salt.

10.1021/bi0609016 CCC: $33.50 
Published on Web 12/02/2006

Scheme 1: Covalent Bond-Breaking and Bond-Forming Reactions That Occur within the Active Site of Glutaryl-CoA Dehydrogenase during the Conversion of Glutaryl-CoA to Crotonyl-CoA[a]

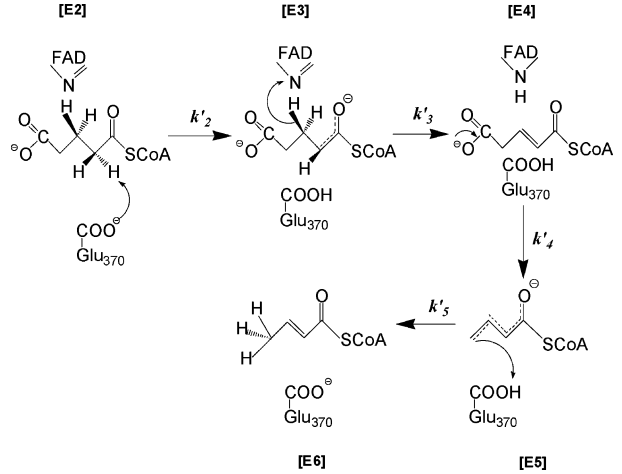


[a] The reoxidation of reduced flavin that occurs by the external electron acceptor is not shown here. E2−E6: each represents an enzyme species with an acyl-CoA intermediate during the progress of reaction with their net rate constants, $k'_2$ to $k'_5$. The binding of the substrate and the release of products are not shown here.

disodium 3-hydroxyglutarate. 3-Hydroxyglutaryl-CoA and glutaconyl-CoA were synthesized using glutaconate CoA-transferase according to Buckel and co-workers and purified (*12*, *13*). A small amount of 3-hydroxyglutaryl-CoA (<2%) is present in glutaconyl-CoA, which possibly arises from either a contaminating or intrinsic hydratase activity of glutaconate-CoA transferase. 2,2,4,4-$d_4$-Glutaryl-CoA and 2,2,3,3,4,4-$d_6$-glutaryl-CoA were synthesized from the acid anhydride as described earlier (*6*). 3-Thiaglutaryl-CoA was synthesized and purified as described (*3*). Purity of the synthetic acyl-CoA esters was assessed by analytical HPLC using the system described by Corkey and modified as described below (*14*). The identity of each acyl-CoA was confirmed by $^1$H NMR and mass spectrometry as described (*6*).

Wild-type and E370Q GCDs were expressed and purified as previously described (*3*). The proteins were quantitated using $\epsilon_{447nm} = 14.5$ and 13.2 $mM^{-1}$ $cm^{-1}$ for the wild-type and E370Q GCDs, respectively (*3*). The numbering of the residues reported here is for the mature human wild-type GCD without the 44 amino acid mitochondrial targeting sequence (NCBI Accession Number Q92947) (*15*). Glutaconate CoA-transferase was prepared as before (*2*, *16*). Protocatechuate 3,4-dioxygenase was a gift from Dr. David Ballou, University of Michigan, Ann Arbor. All other reagents were obtained from commercial sources and were the best grade available.

*Enzyme Assays and Steady-State Kinetics.* GCD activity was routinely assayed using 15−25 nM enzyme at 25 °C in 50 mM potassium phosphate buffer, pH 7.6, 30 $\mu$M glutaryl-CoA and 450 $\mu$M $FcPF_6$ as the electron acceptor, using $\epsilon_{300nm} = 4.3$ $mM^{-1}cm^{-1}$ (*3*).

In steady-state kinetic experiments, glutaryl-CoA was varied (proteo-, 2,2,4,4-$d_4$-, or 2,2,3,3,4,4-$d_6$-glutaryl-CoA) and the steady-state constants determined by nonlinear least-squares fit to the Michaelis−Menten equation using KaleidaGraph 3.6. The deuterium kinetic isotope effects were calculated from these constants as a function of pH. The acyl-CoA product of the steady-state turnover with wild-type has been identified by analytical HPLC as described below.

The steady-state decarboxylation of glutaconyl-CoA (75 $\mu$M) was assayed with 15 nM wild-type GCD at 25 °C in 50 mM potassium phosphate buffer, pH 7.6 over 500 s in a 2.5 mL reaction with constant stirring. Aliquots (160 $\mu$L) of the reaction mixture were quenched at the times indicated by addition of 80 $\mu$L of 95 mM phosphoric acid to bring the pH to 3.4. The precipitated enzyme was removed using a Microcon YM-30 membrane filter, and the filtrate was stored at −80 °C for HPLC analysis. The products were analyzed by injecting 200 $\mu$L of the filtrate onto the HPLC column. The decrease of glutaconyl-CoA and increase in crotonyl-CoA was monitored by HPLC (Beckman System Gold model 126) using a Hypersil C18 analytical column (5 $\mu$m particles; 250 × 4.6 mm) (Phenomenex) with a slight modification of the method of Corkey (*14*). The elution was monitored at 260 nm. The loading and elution was performed at a 0.56 mL/min flow rate with 7.5% solvent B (solvent A is a 100 mM phosphate buffer, pH 5.0; solvent B consists of 40% acetonitrile (v/v) in 100 mM phosphate buffer, pH 5.0). The flow rate was increased from 0.56 to 1.16 mL/min between 2 and 3 min. A linear gradient of 7.5 to 15.0% solvent B was applied during 3−7 min. Isocratic elution was maintained at 15.0% solvent B during 7−12 min. Again, a linear gradient of 15.0−57.5% solvent B was applied during 12−32 min. All the acyl-CoA thioesters eluted within this time period. Acyl-CoA thioesters and their retention times (min) were as follows (average ± standard deviation; $n$ = number of data points): 3-hydroxyglutaryl-CoA, 14.15 ± 0.07 ($n$ = 16); glutaryl-CoA, 18.68 ± 0.22 ($n$ = 16); glutaconyl-CoA, 16.20 ± 0.27 ($n$ = 20); 3-hydroxybutyryl-CoA, 19.30 ± 0.12 ($n$ = 22); crotonyl-CoA, 24.89 ± 0.07 ($n$ = 16). Under these conditions, FAD eluted at 22.77 ± 0.11 min ($n$ = 9). The concentrations of glutaconyl-CoA and crotonyl-CoA were determined from calibration curves relating the concentration of glutaconyl-CoA and crotonyl-CoA to the areas under the curve.

*Rapid Kinetics.* Rapid kinetic reaction measurements were made with an Applied Photophysics SX.18MV Stopped Flow Reaction Analyzer equipped with either a single-wavelength absorption photomultiplier or a 256 element photodiode array detector, as described earlier (*17*). The experiments were setup with over-sampling mode, wherein the instrument collects data at its fastest possible rate. Over-sampling improves the signal-to-noise ratio because there is no danger of distorting kinetic traces. Fits of the data to the appropriate rate equations and evaluation of rate constants were made with the software supplied by Applied Photophysics. For reactions run anaerobically, the stopped flow apparatus was made anaerobic by soaking the syringe assembly with 0.1 M sodium dithionite in 0.1 M dibasic sodium phosphate for 2−3 h followed by a thorough wash with 50 mM potassium phosphate buffer, pH 7.6 that had been bubbled with argon. The rate constant for abstraction of the α-proton from glutaryl-CoA was determined using the substrate analogue, 3-thiaglutaryl-CoA. Enolate formation yields a charge-transfer species with a $\lambda_{max}$ at ~825 nm (*3*). Pseudo-first-order rate constants of the reductive and oxidative half-reactions were determined under anaerobic conditions. All the samples were made anaerobic as described earlier and

Table 1: Deuterium Kinetic Isotope Effects in the Steady State and the Reductive Half-Reaction of Wild-Type Glutaryl-CoA Dehydrogenase as a Function of pH[a]

| pH | kinetic parameter | proteo-glutaryl-CoA | 2,2,4,4-$d_4$-glutaryl-CoA | 2,2,3,3,4,4-$d_6$-glutaryl-CoA |
|---|---|---|---|---|
| 6.5 | $k_{cat}$ ($s^{-1}$) | 5.6 ± 0.2 | 3.7 ± 0.1 | 2.2 ± 0.1 |
| | $^D(k_{cat})$ | | 1.51 | 2.54 |
| | $K_m$ ($\mu$M) | 4.7 ± 1.2 | 5.2 ± 0.9 | 4.8 ± 0.8 |
| | $^D(K_m)$ | | 0.90 | 0.98 |
| | $k_{red}$ ($s^{-1}$) | 20.4 ± 1.0 | 13.3 ± 0.9 | 5.4 ± 0.6 |
| | $^D(k_{red})$ | | 1.53 | 3.75 |
| 7.6 | $k_{cat}$ ($s^{-1}$) | 11.3 ± 0.2 | 7.7 ± 0.1 | 7.2 ± 0.2 |
| | $^D(k_{cat})$ | | 1.47 | 1.57 |
| | $K_m$ ($\mu$M) | 8.1 ± 0.5 | 9.4 ± 0.5 | 9.1 ± 0.9 |
| | $^D(K_m)$ | | 0.86 | 0.89 |
| | $k_{red}$ ($s^{-1}$) | 47.6 ± 2.9 | 25.4 ± 1.5 | 9.9 ± 0.8 |
| | $^D(k_{red})$ | | 1.88 | 4.81 |
| 8.5 | $k_{cat}$ ($s^{-1}$) | 13.2 ± 0.6 | 12.9 ± 0.6 | 9.6 ± 0.6 |
| | $^D(k_{cat})$ | | 1.02 | 1.37 |
| | $K_m$ ($\mu$M) | 34.0 ± 5.3 | 39.3 ± 6.4 | 36.7 ± 7.1 |
| | $^D(K_m)$ | | 0.86 | 0.93 |
| | $k_{red}$ ($s^{-1}$) | 27.9 ± 1.9 | 15.3 ± 0.8 | 7.3 ± 0.7 |
| | $^D(k_{red})$ | | 1.82 | 3.80 |

[a] pH 6.5 was 50 mM phosphate buffer, and pH 8.5 was 2-amino-2-methyl-1,3-propanediol buffer with added KCl to maintain constant ionic strength equal to that of 50 mM phosphate buffer, pH 7.6.

Table 2: Kinetic Rate Constants[a] for the Steady-State Turnover, the Chemical, and Electron-Transfer Steps in the Oxidation of Glutaryl-CoA by Wild-Type Glutaryl-CoA Dehydrogenase

| reaction | wild-type GCD ($s^{-1}$) |
|---|---|
| Steady State | |
| turnover | 5.6 ± 0.3 |
| decarboxylation | 5.5 ± 0.3 |
| Chemical Steps | |
| proton abstraction[b] | 337.2 ± 37.5 |
| hydride transfer | 47.6 ± 2.9 |
| decarboxylation[c] | |
| protonation at C4 | not determined |
| Oxidation of $FADH_2$[d] | |
| first electron | 34.0 ± 13.0 |
| second electron | 235.0 ± 23.0 |

[a] Rate constants are actually "net rate constants" in the forward direction (*7*, *10*). The experiments were performed at 25 °C in 50 mM potassium phosphate buffer, pH 7.6. [b] Rate constant measured using 3-thiaglutaryl-CoA. [c] 28.6 ± 4.7 $s^{-1}$ for decarboxylation of glutaconyl-CoA with E370Q GCD. The rate constants are averages of multiple determinations over different time scales. [d] Performed at 4 °C with ferrocenium hexafluorophosphate as the external electron acceptor.

transferred to the stopped flow apparatus using a gas tight syringe (*2*, *18*). The reductive half-reaction of the flavin by substrate was monitored at 446 nm under pseudo-first-order conditions at 25 °C. The deuterium kinetic isotope effect on the reductive half-reaction was calculated using proteo-, 2,2,4,4-$d_4$-, or 2,2,3,3,4,4-$d_6$-glutaryl-CoA.

The rate constants for the oxidative half-reactions of the dehydrogenase flavin were determined at 4 °C following the increase in absorbance at 446 or 447 nm of the $2e^-$-reduced (hydroquinone) GCD when rapidly mixed with $FcPF_6$. The $2e^-$-reduced protein was generated by anaerobic reduction of the dehydrogenase with 1 equiv of glutaryl-CoA per flavin. The kinetics of reoxidation of the $1e^-$-reduced dehydrogenase was monitored by following the increase in absorbance at 447 nm of the anionic flavin semiquinone of the dehydrogenase that is stabilized by crotonyl-CoA. The flavin semiquinone was generated by photoreduction of the dehydrogenase/crotonyl-CoA complex (at a 1.0:1.1 ratio) under anaerobic conditions in the presence of 10 mM EDTA and 0.5 $\mu$M 5-deazariboflavin (*3*, *19*).

*Miscellaneous Methods.* Absorption spectra were determined using a Shimadzu UV-2401 spectrophotometer or a Hewlett-Packard 8452A diode array spectrophotometer. Mass spectra were determined in the University of Colorado Health Sciences Center Cancer Center using a PE Sciex API-3000 triple quadrupole mass spectrometer.

## RESULTS

*Deuterium Kinetic Isotope Effects.* Consistent with previous work, the steady-state turnover of human GCD at pH 7.6 is 11.3 $s^{-1}$ based on the $1e^-$ reduction of $FcPF_6$ (Table 1) (*3*). Expressed as the turnover of glutaryl-CoA, a $2e^-$ oxidation and decarboxylation, $k_{cat}$ is 5.6 $s^{-1}$ at pH 7.6, whereas the $K_m$ is about 8 $\mu$M (Table 1 and 2). The deuterium kinetic isotope effects on the reactions of 2,2,4,4-$d_4$-glutaryl-CoA and 2,2,3,3,4,4-$d_6$-glutaryl-CoA with wild-type GCD were determined in the steady state and reductive half-reaction of the flavin in the pre-steady state. The data are shown in Table 1. In the steady state, $^D(k_{cat})$ using 2,2,4,4-$d_4$-glutaryl-CoA and 2,2,3,3,4,4-$d_6$-glutaryl-CoA as substrates with wild-type GCD was 1.5 and 1.6, respectively at pH 7.6. A fully expressed primary deuterium kinetic isotope effect is expected to have an upper limit of 7−10 at 25 °C (*20*). A fully expressed kinetic isotope effect on $k_{cat}$ was absent over the pH range studied (pH 6.5−8.5), suggesting that neither proton transfer from C2 nor hydride transfer from C3 to the flavin is rate-determining in the steady state (Table 1). The mechanism of GCD involves two more steps: (i) decarboxylation and (ii) protonation of dienolate anion. Because reprotonation of the transient crotonyl-CoA dienolate anion occurs by solvent-derived protons, neither $d_4$- nor $d_6$-glutaryl-CoA substrates show evidence of an isotope effect (primary or secondary) on the reprotonation reaction in the steady state (*6*). This is not surprising because proton transfer to water from a carboxylic acid is rapid with a diffusive encounter and is not affected by isotope substitutions (*21*). The $^D(K_m)$ is unaltered over the entire pH range for both the substrates with wild-type GCD.

In the pre-steady state, isotope effects on individual chemical steps of bond-breaking and bond-forming events provide better understanding of the reaction mechanism than isotope effects on the steady-state kinetic constants. Stopped flow experiments were conducted under pseudo-first-order conditions for the reductive half-reaction of GCD flavin with proteo-, $d_4$-, and $d_6$-glutaryl-CoA as substrates under anaerobic conditions. The resulting first-order rate constant, $k_{red}$, is used to evaluate the isotope effects. Studying the reductive half-reaction with 2,2,4,4-$d_4$-glutaryl-CoA can only reveal isotope effects on the proton abstraction step that is reflected in changes in the reductive half-reaction; in contrast, with 2,2,3,3,4,4-$d_6$-glutaryl-CoA, isotope effects on both proton abstraction and hydride transfer steps must be observable. The results are shown in Table 1. Again, deuterium kinetic isotope effects on $k_{red}$ are not fully expressed in the pH range 6.5−8.5. The initial proton abstraction step does not contribute significantly to the kinetics of steady-state turnover. $^D(k_{red})$ shows a maximum value of 4.81 at pH 7.6 for the reductive half-reaction of wild-type GCD with $d_6$-glutaryl-

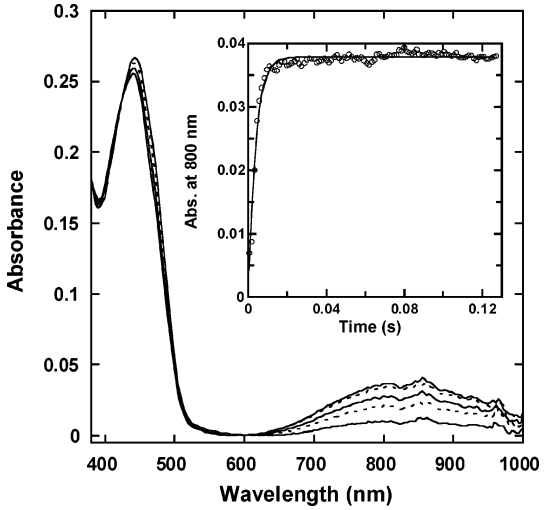


FIGURE 1: Stopped flow data of abstraction of the α-proton of 3-thiaglutaryl-CoA by GCD. (A) Spectra were generated using 20 $\mu$M wild-type GCD and 115 $\mu$M 3-thiaglutaryl-CoA (final concentrations) over 127.4 ms. Over-sampling resulted in collection of 100 spectra over 127.4 ms. Representative spectra shown are at 1.92, 3.2, 4.48, 8.32, and 127.4 ms. Inset: absorbance data at 800 nm analyzed as a first-order reaction. Data have been analyzed as a first-order reaction in the 1−50 ms region. The experiments were performed at 25 °C in 50 mM phosphate buffer, pH 7.6 using a diode-array detector.

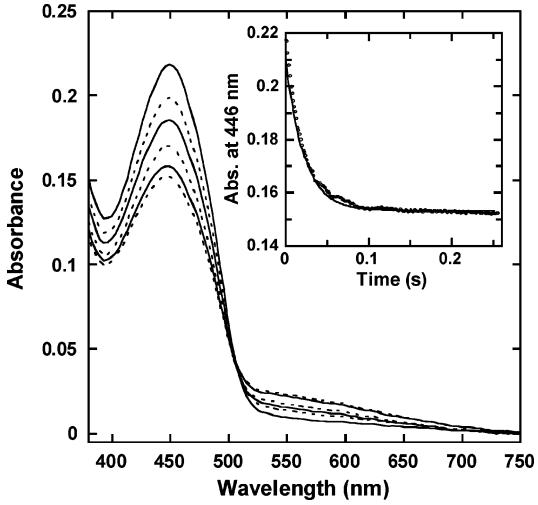


FIGURE 2: Stopped flow data of the reductive half-reaction of hydride transfer from glutaryl-CoA to GCD under anaerobic conditions. Anaerobic condition was maintained by the oxygen-scavenging system using protocatechuate dioxygenase. (A) Spectra were generated using 17.2 $\mu$M wild-type GCD and 150 $\mu$M glutaryl-CoA (final concentrations) over 300 ms. Over-sampling resulted in collection of 200 spectra over 255.4 ms. Representative spectra shown are at 1.92, 8.32, 14.72, 27.52, 65.92, and 255.4 ms. Inset: absorbance data at 446 nm analyzed as a first-order reaction. The experiments were performed at 25 °C in 50 mM phosphate buffer, pH 7.5 with 5% ethylene glycol using a diode-array detector.

CoA as substrate. In the pre-steady-state dehydrogenation reaction, the deuterium kinetic isotope effect would be (a) additive if the proton abstraction and hydride transfer steps were either asynchronous with definitive intermediates or (b) multiplicative if the two steps were either concerted or synchronous with a single intermediate (*22*, *23*). The other possibility is that the transient state kinetic isotope effect is the arithmetic product of the intrinsic isotope effect of all the preceding steps (*22*). However, the isotope effect data do not permit us to distinguish between these possibilities. It is clear that proton abstraction and hydride transfer are not rate-determining in the steady state. Partial contribution of these reactions in the steady state cannot be ruled out. Thus, pre-steady-state kinetic analysis of the individual chemical steps is used to identify the rate-determining step.

*Kinetics of Glutaryl-CoA Dehydrogenase Chemical Steps and Steady-State Decarboxylation.* The deprotonation of glutaryl-CoA at C2 could not be resolved spectrally with wild-type GCD under pre-steady state. Therefore, we estimated the rate constant for the abstraction of the substrate α-proton from the deprotonation of the non-oxidizable substrate analogue, 3-thiaglutaryl-CoA, following the changes across all wavelengths (∼380−900 nm) for the wild-type GCD (Figure 1). The rate constant for formation of the enolate of 3-thiaglutaryl-CoA by the wild-type GCD is 337 $s^{-1}$ (Table 2), much larger than the steady-state turnover rate.

The pre-steady-state kinetics of flavin reduction of wild-type GCD by glutaryl-CoA was studied under anaerobic conditions. The pseudo-first-order rate constant for flavin reduction, i.e., hydride transfer, is 47.6 $s^{-1}$ (Figure 2, Table 2). This rate constant is greater than the turnover rate and, hence, is not rate-determining in the steady state. Also, flavin reduction, which follows the proton abstraction, is much slower than the proton abstraction. The results suggest these two steps are not obligatorily coupled and occur as separate chemical events.

Glutaconyl-CoA is the enzyme-bound intermediate in the conversion of glutaryl-CoA to crotonyl-CoA and $CO_2$ (*2*). The dienolate intermediate observed upon decarboxylation of glutaconyl-CoA could be detected with E370Q GCD because the crotonyl-CoA dienolate forms a charge-transfer complex ($\lambda_{max} \approx 726$ nm) with the oxidized FAD and the substitution of a glutamine residue for Glu370 prevents rapid protonation of the dienolate. The charge-transfer complex was not detected with wild-type GCD in the stopped flow spectrophotometer, likely due to rapid protonation of the dienolate. The substitution of an amide side chain for a carboxylic acid group is conservative because the replacement is isoelectronic (−COOH to $-CONH_2$), isosteric, uncharged but polar, and comparable in its residue volume. Thus, glutamine is a good analogue for the protonated state of glutamate, Glu370($H^+$), which is the state of the catalytic base during the decarboxylation reaction in the regular turnover (Scheme 1). Figure 3A shows the increase in absorbance of the charge-transfer species of E370Q with the dienolate formed upon decarboxylation of glutaconyl-CoA under pseudo-first-order conditions. The data are minimally described using a model with two sequential reactions. The two rate constants are 28.6 ± 4.7 and 3.4 ± 1.6 $s^{-1}$, respectively. The two-step process may reflect (a) an initial decarboxylation reaction with formation of a charge-transfer species, which represents the Cγ−Cδ bond-breaking process, followed by (b) a subtle internal conformational change in the active site to maximize the orbital overlap, leading to a much more intense charge-transfer band. The second slower step appears to be irrelevant in catalysis. The characteristics of these distinct spectral species are (a) higher intensity of the charge-transfer band and (b) a blue shift in the 450 nm transition of the flavin chromophore (Figure 3B). The decay of the charge-transfer species, presumably reflecting proto-

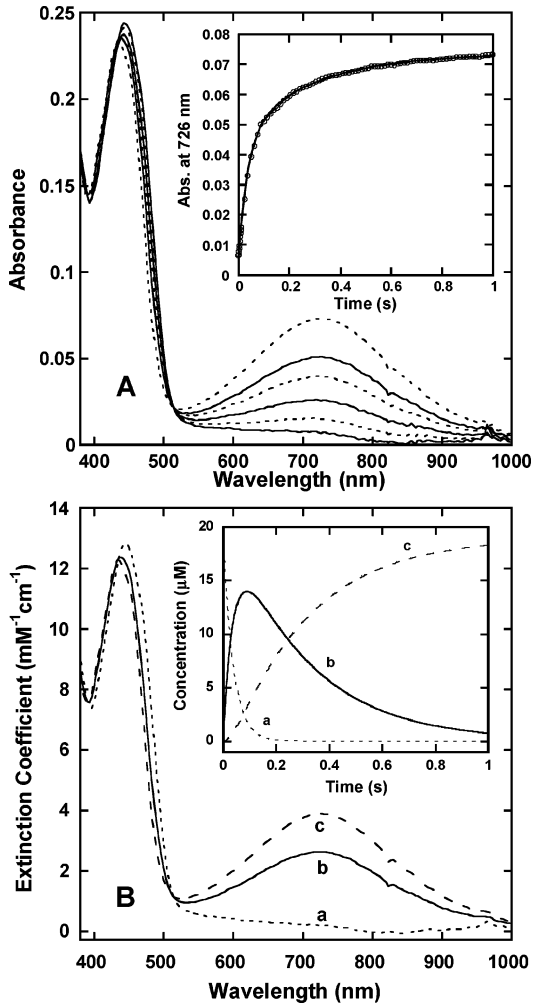


FIGURE 3: Stopped flow data of decarboxylation reaction of glutaconyl-CoA by GCD. (A) Spectra were generated using 19 $\mu$M E370Q GCD and 400 $\mu$M glutaconyl-CoA (final concentrations) over 1000 ms. Over-sampling resulted in collection of 800 spectra over 1023 ms. Representative spectra shown are at 1.92, 10.08, 24.96, 50.56, 100.5, and 1023 ms. Inset: absorbance data at 726 nm analyzed as two sequential first-order reactions. (B) Computed spectral species of the three components a, b, and c. Inset: computed kinetic profiles of the three spectral species a, b, and c. The experiments were performed at 25 °C in 50 mM phosphate buffer, pH 7.6 using a diode-array detector.

nation of the crotonyl-CoA dienolate, lies beyond the time scale of this experiment with E370Q GCD.

In the steady state, wild-type GCD catalyzes the decarboxylation of glutaconyl-CoA with an apparent $k_{cat}$ of 5.5 $s^{-1}$, expressed as a turnover number (Figure 4, Table 2). The reaction conditions used, 75 $\mu$M glutaconyl-CoA with 15 nM GCD, imply that the reaction is under steady state because the $K_m$ of glutaconyl-CoA with wild-type GCD in the hydratase reaction is about 3 $\mu$M and the $K_i$ is about 1.0 $\mu$M as a competitive inhibitor of the dehydrogenase (*2*). The product of decarboxylation of glutaconyl-CoA by wild-type GCD has been confirmed to be crotonyl-CoA by HPLC. The rate of depletion of glutaconyl-CoA is identical to the rate of appearance of crotonyl-CoA. These experiments showed that the steady-state rate of glutaconyl-CoA decarboxylation by wild-type GCD is equal to the steady-state turnover of glutaryl-CoA oxidation and decarboxylation. Moreover, the product of turnover of glutaryl-CoA by wild-type GCD is known to be crotonyl-CoA. That the overall steady-state rate

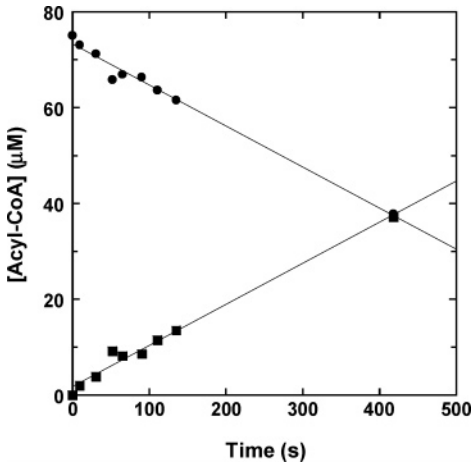


FIGURE 4: Steady-state decarboxylation of glutaconyl-CoA (75 $\mu$M) using wild-type GCD (15 nM). Depletion of glutaconyl-CoA (●) and concomitant formation of crotonyl-CoA (■) was monitored using analytical HPLC. The slope of the straight line represents the maximum velocity of the decarboxylation reaction.

is identical to the steady-state rate of glutaconyl-CoA decarboxylation indicates that the release of crotonyl-CoA, the product with both the reactions, is rate-determining in the steady state. This is consistent with the finding that the deuterium kinetic isotope effects are not fully expressed in the steady state.

Electron transfer from acyl-CoA dehydrogenases to their physiological electron acceptor, an electron-transfer flavoprotein, occurs in two $1e^-$ steps, and the rates for electron transfers to $FcPF_6$ from $1e^-$- and $2e^-$-reduced medium-chain acyl-CoA dehydrogenases have been determined by Lehman and Thorpe (*24*). Unlike the case with medium-chain acyl-CoA dehydrogenases, near quantitative generation of a $2e^-$-reduced state of GCD does not occur with a stoichiometric amount of substrate. A large excess of glutaryl-CoA would be required to quantitatively generate $2e^-$-reduced GCD, which would lead to multiple turnovers and complicate interpretation of the results. Therefore, the wild-type GCD was reduced with equimolar substrate, which was then reoxidized by $FcPF_6$ in the stopped flow spectrophotometer at 4 °C. The large rate constant expected for this oxidation necessitated working at a lower temperature for the detection of spectral species. The oxidation of the $2e^-$-reduced wild-type GCD/glutaryl-CoA complex was best fit to a sum of two exponentials with $k_1 = 235 \pm 23$ $s^{-1}$ and $k_2 = 34 \pm 13$ $s^{-1}$ (Figure 5). The rate constant for oxidation of the $1e^-$-photochemically-reduced semiquinone wild-type dehydrogenase with bound crotonyl-CoA is $267 \pm 25$ $s^{-1}$ (Figure 5). Thus, it may be inferred that the slower step is the transfer of the first electron from the $2e^-$-reduced wild-type dehydrogenase. The faster step is oxidation of the $1e^-$-reduced semiquinone state. Similar results were obtained with the medium-chain acyl-CoA dehydrogenase upon oxidation of the substrate-reduced enzyme by $FcPF_6$ (*24*). Saenger and co-workers have established that the binding of thioesters regulates the reoxidation of acyl-CoA dehydrogenases (*25*). Thus, oxidation of reduced FAD is much faster than the chemical steps that occur in the active site of the enzyme. The rapid rate of oxidation of reduced FAD may lead to rate enhancement of the decarboxylation reaction.

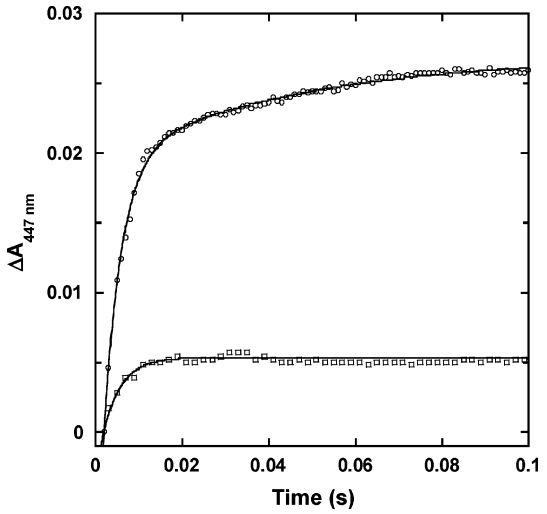


FIGURE 5: Stopped flow data of change in absorbance at 447 nm due to oxidation of either hydroquinone (2e$^-$-reduced) or semiquinone (1e$^-$-reduced) state of flavin of GCD by ferrocenium hexafluorophosphate under anaerobic conditions. Wild-type GCD hydroquinone (15 $\mu$M) (reduced by stoichiometric equivalent of glutaryl-CoA) (○) was oxidized by 200 $\mu$M $FcPF_6$ over 100 ms. Absorbance data at 447 nm were analyzed as two sequential first-order reactions. Similarly, 12 $\mu$M wild-type GCD semiquinone in the presence of crotonyl-CoA (photochemically reduced) (□) was oxidized by 200 $\mu$M $FcPF_6$ over 100 ms. Absorbance data at 447 nm were analyzed as a first-order reaction. The experiments were performed at 4 °C in 50 mM phosphate buffer, pH 7.6 using a single-wavelength absorption photomultiplier detector. Only final concentrations of reagents are reported.

## DISCUSSION

The kinetic mechanism of glutaryl-CoA dehydrogenase involves several physical, chemical, and electron-transfer steps: (a) binding of glutaryl-CoA substrate to the oxidized form of the enzyme; (b) abstraction of the α-proton of the substrate by the catalytic base, Glu370; (c) hydride transfer from the $\beta$-carbon of the substrate to the N(5) of the FAD, yielding the 2e$^-$-reduced form of FAD; (d) decarboxylation of glutaconyl-CoA, an enzyme-bound intermediate, by breaking the C$\gamma$−C$\delta$ bond, resulting in formation of a dienolate anion, a proton, and $CO_2$; (e) protonation of the dienolate intermediate, resulting in crotonyl-CoA product formation; (f) release of products from the active site; and (g) oxidation of the 2e$^-$-reduced form of FAD in two 1e$^-$ steps by an external electron acceptor to complete the turnover. Scheme 1 represents the chemical steps (b) to (e) that occur within the active site of the enzyme. The intermolecular electron transfer (g) occurs at the surface of the enzyme by an external electron acceptor (*9*). The physical steps of substrate binding and product release refer to (a) and (f), respectively. An effort has been made here to identify the rate-determining step in the steady-state turnover of wild-type GCD by studying deuterium kinetic isotope effects and transient state kinetics. The overall reaction is irreversible, owing to the decarboxylation step and the use of an artificial electron acceptor, $FcPF_6$. Ferrocenium renders the oxidation steps essentially irreversible due to the potential of the electron acceptor, ~380 mV (*24*).

With GCD, deuterium kinetic isotope effects were not fully expressed with either of the substrates, $d_4$- and $d_6$-glutaryl-CoA, over a range of pH values, indicating that none of the chemical steps in the oxidation of glutaryl-CoA are completely rate-determining in the steady state. In comparison, the oxidation of butyryl-CoA by medium-chain acyl-CoA dehydrogenase appears to be a concerted reaction for proton abstraction and hydride transfer because fully expressed deuterium kinetic isotope effects that are multiplicative for the two steps are seen (*23*). It is unknown whether oxidation of octanoyl-CoA, the optimal substrate, is concerted; however, a recent computational approach with octanoyl-CoA as substrate suggests that the two C−H bond-breaking steps are not concerted (*26*). Computational studies with short-chain acyl-CoA dehydrogenase suggest that the proton abstraction by the catalytic base is followed by hydride transfer to N(5) of FAD and that the two steps are not concerted or are, at best, consistent with an asynchronous, concerted reaction (*27*), although there is no experimental evidence. (An unpublished thesis reports kinetic isotope effects of 1.2−2.2 for different substitutions on butyryl-CoA with short-chain acyl-CoA dehydrogenase; please see ref 26 for details). Our data with GCD suggest that none of the chemical steps are completely rate-determining in the steady-state turnover. Therefore, transient state kinetics, in conjunction with transit time analysis, has been used to identify the rate-determining step in the steady-state turnover of GCD.

Scheme 2: The Sequence of Enzyme Species in the Overall Turnover of Glutaryl-CoA Dehydrogenase[a]

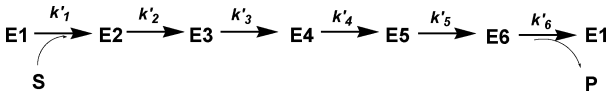


[a] E1 refers to the uncomplexed, oxidized form of the enzyme. E2−E6 refer to enzyme forms that are bound with an acyl-CoA as represented by the four chemical steps that occur within their active sites (for details, please see Scheme 1). E1 is regenerated by release of product from E6. The associated net rate constants in the forward direction are $k'_1$−$k'_6$ (*7*).

*Transit Time Analyses Using Net Rate Constants and Identification of the Rate-Determining Step in the Steady-State Turnover of Wild-Type Glutaryl-CoA Dehydrogenase.* In the steady state, the turnover number for the overall reaction of GCD and the decarboxylation of the enzyme-bound intermediate, glutaconyl-CoA, have identical rate constants, 5.6 and 5.5 $s^{-1}$, respectively. Crotonyl-CoA is the product generated in both of these steady-state reactions. The transit time for a single turnover under steady-state conditions for either reaction, i.e., oxidation and decarboxylation of glutaryl-CoA or decarboxylation of glutaconyl-CoA, is ~ 180 milliseconds ($1/k_{cat}$) (*10*).

The sequence of steps occurring within the active site of GCD may be written as follows (Scheme 2). Here, E1 refers to the uncomplexed, oxidized form of the enzyme; E2−E6 refer to enzyme forms that are bound with an acyl-CoA, representing chemical steps (b)−(e) that occur within their active sites (Scheme 1). Scheme 1 shows the conversion of glutaryl-CoA to crotonyl-CoA, which occurs within the active site of the enzyme. Each covalent bond-breaking and bond-forming event is depicted. The reoxidation of reduced flavin that occurs by the external electron transfer to ferrocenium is not shown here. In Scheme 2, the associated net rate constants are $k'_1$ to $k'_6$ (*7*). Scheme 1 shows the net rate constants, $k'_2$ to $k'_5$, associated with the chemical steps.

In a set of sequential steps, the transit time for a single turnover under steady state (for the overall reaction) must equal the sum of the transit times of each of the chemical

steps and the physical steps occurring within the active site or the electron-transfer steps that occur away from the active site but those that are involved in a complete cycle (*10*).

$$\frac{1}{k_{cat}} = \frac{1}{k'_1} + \frac{1}{k'_2} + \frac{1}{k'_3} + \frac{1}{k'_4} + \frac{1}{k'_5} + \frac{1}{k'_6}$$

From Table 2, adding the transit times for all the discernible events in a turnover, we arrive at a total time of ~59 milliseconds (= 1/337.2 + 1/47.6 + 1/28.6) in comparison to ~180 milliseconds for a steady-state transit time, i.e., ~33%. The reoxidation of the GCD flavin occurs externally to the active site and in parallel with the active site chemistry. The upper limit for the transit time for external electron-transfer steps is ~34 milliseconds in the absence of any correction for temperature. The electron-transfer steps are not rate-determining in the steady-state turnover and therefore need not be included in computing the cumulative transit time. The physical and chemical steps that occur within the active site are included in the transit time analysis.

It is clear that we do not account for a significant portion, ~67%, of the transit time. Thus, the discerned chemical steps and the electron-transfer steps are insufficient to account for the steady-state transit time. The following steps in catalysis have not been included in the evaluation of the cumulative transit time: (a) protonation at C$\gamma$ of the crotonyl-CoA dienolate intermediate resulting in crotonyl-CoA product, (b) the physical steps of binding of the substrate, and (c) release of the products: crotonyl-CoA, $CO_2$, and a proton. We have referred to "product release" instead of "product dissociation" to include any conformational changes associated with product dissociation so as to not distinguish between these two physical processes (*10*).

The release of $CO_2$ and the proton are assumed to be rapid and not kinetically significant in the steady-state reaction because $CO_2$ and the proton are not likely to be tightly held in the active site and can dissociate from the active site of the enzyme by diffusion. It is not required to consider the physical step of formation of the ES complex in the transit time analysis of a turnover with net rate constants, although it is assumed to be a diffusion-encountered process on the order of $10^8$ $M^{-1}$ $s^{-1}$ (*10*), or $k_{cat}/K_m$ (~$6.8 \times 10^5$ $M^{-1}$ $s^{-1}$) may be considered as an apparent second-order rate constant for substrate binding. In either case, substrate binding would be very fast and insufficient to account for the steady-state transit time. It has not been possible to directly evaluate the kinetics of the chemical step of protonation of the dienolate anion at C4, formed upon decarboxylation of glutaconyl-CoA. However, an estimate of the upper and lower limits of the rate constant for protonation of the dienolate anion may be provided. In the decarboxylation reaction of glutaconyl-CoA, monitored by stopped flow spectrophotometry, with wild-type GCD, the charge-transfer species could not be observed on a 20 ms time scale or longer, whereas the product analyses (reaction performed by stop−quench method, and products analyzed by analytical HPLC) showed 100% conversion of glutaconyl-CoA to crotonyl-CoA, implying that the true rate constant is at least 50 $s^{-1}$ (Rao, Albro, and Frerman, unpublished results). Therefore, the true rate constant of protonation of the dienolate anion lies between 50 and ~300 $s^{-1}$. The upper limit is the rate constant for α-proton abstraction from 3-thiaglutaryl-CoA catalyzed by wild-type GCD because Glu370 is positioned to catalyze rapid proton transfers at C2 and C4 positions (Table 2) (*5*, *6*, *17*). The only other physical step, which is crotonyl-CoA product release, remains to be addressed. The rate constant for proton exchange at C4 catalyzed by wild-type GCD with crotonyl-CoA is 9.8 $s^{-1}$ at 25 °C (*6*). The exchange reaction involves multiple binding and release events along with C−H bond-breaking and C−D bond-forming events at the C4 position of crotonyl-CoA. Also, proton−deuteron exchange is proposed to be mediated by the catalytic base at the level of Glu370($H^+$) (*6*). Arguments much like the ones described above rule out the possibility that the chemical steps of bond-breaking and bond-forming reactions are slow, suggesting that the exchange rate constant reflects the rate constant of release of crotonyl-CoA from the active site.

The total transit time for a turnover may now be computed from the individual steps:

$$\frac{1}{337.2} + \frac{1}{47.6} + \frac{1}{28.6} + \frac{1}{50} + \frac{1}{9.8} = \frac{1}{5.52}$$

The net rate constants are taken from Table 2, estimated from a preliminary experiment and from a previous publication (*6*). Therefore, the total transit time for a turnover is ~181 milliseconds, allowing us to compute a $k_{cat}$ of 5.52 $s^{-1}$. The computed $k_{cat}$ compares very well with that of the steady-state turnover of glutaryl-CoA oxidation and decarboxylation (5.6 ± 0.3 $s^{-1}$) and with the steady-state decarboxylation of glutaconyl-CoA (5.5 ± 0.3 $s^{-1}$) at pH 7.60 (Table 2). It is clear that the major rate-determining step in the steady-state turnover of wild-type GCD is crotonyl-CoA release. The computed transit time for the decarboxylation reaction of glutaconyl-CoA by GCD is ~157 milliseconds, yielding a rate constant of ~6.4 $s^{-1}$. We consider this computed rate constant for decarboxylation as being comparable to the experimentally derived steady-state decarboxylation rate of 5.5 ± 0.3 $s^{-1}$ (Table 2). It is clear that the rate of release of crotonyl-CoA accounts for about 56% of the steady-state turnover rate, whereas all other processes put together account for the remaining 44%. Thus, product release is the major rate-determining step, whereas the steps preceding it are partially rate-determining. The transit time for the oxidation of glutaryl-CoA to glutaconyl-CoA and its decarboxylation account for about 13% and 31%, respectively.

In the single turnover of glutaryl-CoA with wild-type GCD, the first-order rate constant of ~12 $s^{-1}$ (11.6 or 11.9 $s^{-1}$; transit time ~84 milliseconds) refers to the slowest chemical step in the entire turnover process or a combination of all the individual rate constants (*6*, *17*). Adding the transit time for H−D exchange at the C4 of crotonyl-CoA ($k_{ex}$ = 9.8 $s^{-1}$; transit time ~102 milliseconds (*6*)) yields a total transit time of 187 ms, which agrees with the transit time for the steady-state turnover (~181 ms). In an earlier work, Rao and co-workers had remarked that, in the single turnover experiment, the rate constant for the depletion of $d_4$-glutaryl-CoA or formation of $d_3$-crotonyl-CoA included all the chemical events but excluded product release (*6*). Transit time analysis for the single turnover experiment is valid because the first-order rate constant of ~12 $s^{-1}$ is with respect to the ES complex and represents a "net rate constant" in the forward direction with the chemical steps occurring

within the active site of GCD. The single turnover experiments were previously reported (*6*) and are internally consistent with the present results.

Transit time analysis requires the isolation of individual chemical events by using substrate analogues and mutant forms of the enzyme to obtain net rate constants that are comparable to the turnover reaction with the wild-type enzyme and normal substrates. The rate constants must be obtained with high precision. The rate constant for the initial α-proton abstraction by GCD is reasonably estimated by using 3-thiaglutaryl-CoA. The arguments in support of this idea compare the equivalence of the α-proton of the substrate analogue, 3-thiaglutaryl-CoA, with that of the enzyme-bound substrate, glutaryl-CoA. The binding of either ligand in the active site of the enzyme is comparable as the two ligands are structurally analogous and yield essentially same $K_m$ or $K_d$ values (*3*). The criteria that determines the rate of proton abstraction is the $\Delta pK_a$ between proton donor (substrate or analogue) and the conjugate acid of the catalytic base (Glu370($H^+$) in our case). The $pK_a$ of the conjugate acid of the catalytic base Glu370($H^+$) is not expected to differ with different ligands, although its value is not known. The $pK_a$ of the α-proton of the substrate analogue, 3-thiaglutaryl-CoA, is 7.0 when bound to the enzyme (*3*), whereas that of the substrate, glutaryl-CoA, is unknown. The $pK_a$ of the α-proton of the substrate is expected to be higher by ∼3−5 pH units in free solution (*28*, *29*) but closer to 7.0 when bound to the enzyme. Because the proton-transfer reaction is neither strongly exothermic nor endothermic when $-4 < \Delta pK_a < 4$ (*30*), the rates of proton abstraction within this $\Delta pK_a$ range would be of the same order of magnitude. Thus, the magnitude of $\Delta pK_a$ with substrate would be close to that with 3-thiaglutaryl-CoA (within ±4 pH units). The rate constant of abstraction of the α-proton from the substrate could be either under- or over-estimated by using 3-thiaglutaryl-CoA. In the extreme case, the lower limit of the rate of proton abstraction from glutaryl-CoA must be at least ∼50 $s^{-1}$, the rate of the hydride transfer reaction (see below). This would yield a transit time of ∼20 ms, which is still only a small part of the transit time for a turnover (∼181 ms), accounting for about 10%. The rate constant with 3-thiaglutaryl-CoA may actually be an under-estimate because the formation of the charge-transfer species with the substrate is not observed. In this case, the transit time the for proton abstraction reaction with glutaryl-CoA would be ≤3 milliseconds, i.e., reciprocal of 337.2 $s^{-1}$ (Table 2). Alternatively, the proton abstraction rate constant may be estimated by transit time analysis of the single turnover experiment by excluding the product release step and using the available data from Table 2 (*6*). The transit time analysis for the single turnover experiment, by assuming the rate constant for protonation of the dienolate to be 50 $s^{-1}$, yields 110 $s^{-1}$. Thus, the estimation of the true rate constant for proton abstraction using 3-thiaglutaryl-CoA seems not unusually large or small.

The rate constant for the protonation of the dienolate may also be estimated by transit time analysis of the single turnover experiment. It is interesting to note that this analysis yields a rate constant for protonation of the dienolate of ∼38.3 $s^{-1}$, which is in reasonable agreement with the estimated rate constant of 50 $s^{-1}$ for this step.

Quantitative structure−activity relationships (QSAR) study with alternate substrates with GCD indicated a large electron demand at the reaction center, implying that the reduction of electron deficient flavin is the dominating factor in the turnover of the enzyme (*31*). QSAR parameters may be correlated to a reaction parameter (equilibrium or rate constants) that represents a linear free energy relationship (*32*). In our QSAR study, $\log(k_{cat})$, which represents an "energy function" related to $\Delta G^{\ddagger}$, was used (*31*). In GCD, the isotope effect is best expressed on the hydride transfer step and the QSAR study indicated a similar conclusion. Therefore, it may be suggested that the highest thermodynamic barrier encountered by the enzyme, in its turnover with substrate, is actually the chemical step of hydride transfer. Thus, the hydride transfer step may be considered the "rate-determining" step in catalysis because this is the step traversing the highest point in an energy profile, according to one of the definitions of a rate-determining step (*33*). The other chemical steps involved in the turnover, deprotonation at Cα, the Cγ−Cδ bond breaking for decarboxylation, and reprotonation at Cγ, must have much lower energy barriers and are partially rate-determining.

## REFERENCES


1. Lenich, A. C., and Goodman, S. I. (1986) The purification and characterization of glutaryl-coenzyme A dehydrogenase from porcine and human liver, *J. Biol. Chem. 261*, 4090−4096.
2. Westover, J. B., Goodman, S. I., and Frerman, F. E. (2001) Binding, Hydration, and Decarboxylation of the Reaction Intermediate Glutaconyl-Coenzyme A by Human Glutaryl-CoA Dehydrogenase, *Biochemistry 40*, 14106−14114.
3. Dwyer, T. M., Rao, K. S., Goodman, S. I., and Frerman, F. E. (2000) Proton Abstraction Reaction, Steady-State Kinetics, and Oxidation−Reduction Potential of Human Glutaryl-CoA Dehydrogenase. *Biochemistry 39*, 11488−11499.
4. Dwyer, T. M., Rao, K. S., Westover, J. B., Kim, J. J., and Frerman, F. E. (2001) The function of Arg-94 in the oxidation and decarboxylation of glutaryl-CoA by human glutaryl-CoA dehydrogenase, *J. Biol. Chem. 276*, 133−138.
5. Fu, Z., Wang, M., Paschke, R., Rao, K. S., Frerman, F. E., and Kim, J. J. (2004) Crystal Structures of Human Glutaryl-CoA Dehydrogenase with and without an Alternate Substrate: Structural Bases of Dehydrogenation and Decarboxylation Reactions, *Biochemistry 43*, 9674−9684.
6. Rao, K. S., Albro, M., Zirrolli, J. A., Vander Velde, D., Jones, D. N., and Frerman, F. E. (2005) Protonation of Crotonyl-CoA Dienolate by Human Glutaryl-CoA Dehydrogenase Occurs by Solvent-Derived Protons, *Biochemistry 44*, 13932−13940.
7. Cleland, W. W. (1975) Partition Analysis and the Concept of Net Rate Constants as Tools in Enzyme Kinetics, *Biochemistry 14*, 3220−3224.
8. Fisher, H. F. (2005) Transient-State Kinetic Approach to Mechanisms of Enzymatic Catalysis, *Acc. Chem. Res. 38*, 157−166.
9. Ghisla, S., and Thorpe, C. (2004) Acyl-CoA dehydrogenases. A mechanistic overview, *Eur. J. Biochem. 271*, 494−508.
10. Fersht, A. (1999) *Structure and Mechanism in Protein Science*: *A Guide to Catalysis and Protein Folding*, W. H. Freeman and Co., New York.
11. Waterson, R. M., and Hill, R. L. (1972) Enoyl coenzyme A hydratase (crotonase). Catalytic properties of crotonase and its possible regulatory role in fatty acid oxidation, *J. Biol. Chem. 247*, 5258−5265.
12. Buckel, W., Dorn, U., and Semmler, R. (1981) Glutaconate CoA-transferase from *Acidaminococcus fermentans*, *Eur. J. Biochem. 118*, 315−321.
13. Klees, A. G., and Buckel, W. (1991) Synthesis and properties of (R)-2-hydroxyglutaryl-1-CoA: (R)-2-hydroxyglutaryl-5-CoA, an erroneous product of glutaconate CoA-transferase, *Biol. Chem. Hoppe−Seyler 372*, 319−324.
14. Corkey, B. E. (1988) Analysis of acyl-coenzyme A esters in biological samples, *Methods Enzymol. 166*, 55−70.

15. Goodman, S. I., Kratz, L. E., DiGiulio, K. A., Biery, B. J., Goodman, K. E., Isaya, G., and Frerman, F. E. (1995) Cloning of glutaryl-CoA dehydrogenase cDNA, and expression of wild type and mutant enzymes in *Escherichia coli*, *Hum. Mol. Genet. 4*, 1493−1498.
16. Mack, M., Bendrat, K., Zelder, O., Eckel, E., Linder, D., and Buckel, W. (1994) Location of the two genes encoding glutaconate coenzyme A-transferase at the beginning of the hydroxyglutarate operon in *Acidaminococcus fermentans*, *Eur. J. Biochem. 226*, 41−51.
17. Rao, K. S., Albro, M., Vockley, J., and Frerman, F. E. (2003) Mechanism-based inactivation of human glutaryl-CoA dehydrogenase by 2-pentynoyl-CoA: rationale for enhanced reactivity, *J. Biol. Chem. 278*, 26342−26350.
18. Patil, P. V., and Ballou, D. P. (2000) The use of protocatechuate dioxygenase for maintaining anaerobic conditions in biochemical experiments, *Anal. Biochem. 286*, 187−192.
19. Massey, V., and Hemmerich, P. (1978) Photoreduction of Flavoproteins and Other Biological Compounds Catalyzed by Deazaflavins, *Biochemistry 17*, 9−16.
20. Glickman, M. H., Wiseman, J. S., and Klinman, J. P. (1994) Extremely Large Isotope Effects in the Soybean Lipoxygenase−Linoleic Acid Reaction, *J. Am. Chem. Soc. 116*, 793−794.
21. Rose, I. A. (1970) *Enzymology of proton abstraction and transfer reactions* in *The Enzymes* (Boyer, P. D., Ed.) 3rd ed., Vol. 2, pp 281−320, Academic Press, New York.
22. Maniscalco, S. J., Tally, J. F., and Fisher, H. F. (2004) The interpretation of multiple-step transient-state kinetic isotope effects, *Arch. Biochem. Biophys. 425*, 165−172.
23. Pohl, B., Raichle, T., and Ghisla, S. (1986) Studies on the reaction mechanism of general acyl-CoA dehydrogenase. Determination of selective isotope effects in the dehydrogenation of butyryl-CoA, *Eur. J. Biochem. 160*, 109−115.
24. Lehman, T. C., and Thorpe, C. (1990) Alternate Electron Acceptors for Medium-Chain Acyl-CoA Dehydrogenase: Use of Ferricenium Salts, *Biochemistry 29*, 10594−10602.
25. Saenger, A. K., Nguyen, T. V., Vockley, J., and Stankovich, M. T. (2005) Thermodynamic Regulation of Human Short-Chain Acyl-CoA Dehydrogenase by Substrate and Product Binding, *Biochemistry 44*, 16043−16053.
26. Bhattacharyya, S., Ma, S., Stankovich, M. T., Truhlar, D. G., and Gao, J. (2005) Potential of Mean Force Calculation for the Proton and Hydride Transfer Reactions Catalyzed by Medium-Chain Acyl-CoA Dehydrogenase: Effect of Mutations on Enzyme Catalysis, *Biochemistry 44*, 16549−16562.
27. Poulsen, T. D., Garcia-Viloca, M., Gao, J. L., and Truhlar, D. G. (2003) Free Energy Surface, Reaction Paths, and Kinetic Isotope Effect of Short-Chain Acyl-CoA Dehydrogenase, *J. Phys. Chem. B 107*, 9567−9578.
28. Bordwell, F. G., Vanderpuy, M., and Vanier, N. R. (1976) Carbon Acids. 9. Effects of Divalent Sulfur and Divalent Oxygen on Carbanion Stabilities, *J. Org. Chem. 41*, 1885−1886.
29. Lau, S. M., Brantley, R. K., and Thorpe, C. (1988) The Reductive Half-Reaction in Acyl-CoA Dehydrogenase from Pig Kidney: Studies with Thiaoctanoyl-CoA and Oxaoctanoyl-CoA Analogues, *Biochemistry 27*, 5089−5095.
30. Kyte, J. (1995) *Mechanism in Protein Chemistry*, Garland Publishing, New York.
31. Rao, K. S., Vander Velde, D., Dwyer, T. M., Goodman, S. I., and Frerman, F. E. (2002) Alternate Substrates of Human Glutaryl-CoA Dehydrogenase: Structure and Reactivity of Substrates, and Identification of a Novel 2-Enoyl-CoA Product, *Biochemistry 41*, 1274−1284.
32. Smith, M. B., and March, J. (2001) *March's Advanced Organic Chemistry: Reactions, Mechanisms, and Structure*, 5th ed., Wiley-Interscience, New York.
33. Cleland, W. W., and Northrop, D. B. (1999) Energetics of substrate binding, catalysis, and product release, *Methods Enzymol. 308*, 3−27.

BI0609016